A Hybrid Numerical-Analytical Method to Evaluate Short-Term Temperatures Changes in Geothermal Boreholes

Carlos Prieto[1] and Massimo Cimmino[1]
[1]Département de génie mécanique, Polytechnique Montréal, Montréal, Canada

Abstract

The simulation of ground-source heat pump systems coupled to vertical geothermal boreholes is typically conducted using spatial and temporal superposition techniques on analytical solutions of the heat equation. While numerical methods offer greater flexibility in bore field configurations and physical processes that can be taken into account, they are seen as computationally inefficient when compared to their analytical counterparts. In the present research, a hybrid model is introduced for the simulation of single U-tube geothermal boreholes, with the U-tube simplified as a single equivalent pipe. The model encompasses a finite difference scheme for time derivatives to simulate heat transfer in the grout and the ground, and an analytical solution to evaluate the fluid temperature and heat transfer rate profiles along the equivalent pipe. The model is compared against a reference finite element model and the experimental data set of Beier et al. (2011).

Introduction

Ground-coupled heat pumps (GCHP) are highly-efficient, energy saving, reliable and environment-friendly systems, the core of which is the ground heat exchanger (GHE). The drilling costs associated with the GHE constitute a major portion of the overall cost of a GCHP system. The efficiency of a GCHP depends on the fluid temperatures within the GHE, and thus the heat transfer modelling of the GHE is critical to the accurate design and operation of GCHP systems. Many heat transfer models have been proposed and can be divided into analytical and numerical models.

In the literature, there are some analytical models, i.e. infinite line source (ILS), finite line source (FLS), infinite cylindrical source (ICS), etc. These methods are used to evaluate temperature changes from heat conduction between the GHE and the soil, with imposed – and often uniform – heat transfer rate applied over the GHE. The common characteristics is that these analytical models ignore the borehole heat capacity providing an inaccurate average fluid temperature for a short time simulation (Lamarche, 2013). Neglecting the borehole thermal capacity leads to an overestimation of the fluid (and ground) temperature changes. This will in turn lead to an underestimation of the system's performance and an overestimation of the required GHE size.

Simplified one-dimensional models have been recommended for GHE design. Several authors have proposed to model the GHE using a single equivalent pipe, rather than including the two (or more) pipes of the GHE. This approach enables the development of closed form analytical solutions for the fluid temperature.

Bose et al. (1985) introduced the equivalent pipe assumption using a conformal mapping technique. Gu and O'Neal (1998), following the work of Bose et al. (1985) developed an analytical expression for the fluid temperature. They solved the steady state heat conduction equation, assuming constant conductivity coefficients independently of the parameters used in the conformal mapping. Both the thermal capacitance of the borehole and the axial heat flow in the grout and pipe walls were neglected, as the authors were not concerned with the short-term temperature variations.

Bandyopadhyay et al. (2008) proposed an analytical solution for the heat transfer into the GHE. In their work, Laplace domain solutions were obtained for the equivalent pipe of the GHE. The calculation of the average fluid temperature was done by means of the Gaver–Stehfest algorithm for inversion of the Laplace domain solution (Stehfest, 1970).

Javed and Claeson (2011) developed a time domain analytical solution to model the short time response of the borehole. The model considers an equivalent pipe with a single average temperature. The influence of the thermal capacity of the grout and fluid is considered but the interactions between legs of the U-tube is neglected. Lamarche (2015) later proposed a technique for the complete inversion of the solution from the Laplace domain to the time domain.

Other authors have proposed the use of numerical methods to evaluate fluid temperatures in the GHE. The single equivalent pipe assumption simplifies the geometry to a one-dimensional problem, thereby reducing the computational complexity of the numerical method.

Shonder and Beck (1999) proposed a numerical method to simulate the heat transfer into the borehole using a single equivalent pipe. The flow in the pipes were modeled as one equivalent flow and the heat capacity was included for modeling heat storage between pipes and fluid. The model is applied to the analysis of field monitored data, and a parameter estimation method is used to estimate the value of the thermal properties of the GHE and the soil (e.g. the thermal conductivities).

Yavuzturk and Spitler (1999) developed a two-dimensional radial-azimuthal finite volume model of a GHE cross-section, with the circular pipes approximated as pie sectors on the two-dimensional grid. The authors generate short time-step g-functions from a constant heat injection rate imposed on the pipes.

Xu and Spliter (2006) developed a one-dimensional finite volume model to simulate the short-term response of a GHE using an equivalent pipe. The fluid is represented by an annular volume within the pipe with equivalent thermal capacity.

A one-dimensional finite volume model is also presented by Brussieux and Bernier (2019). The authors coupled the numerical model, representing the fluid, the pipe and the grout, to the analytical cylindrical heat source to represent the soil. The model was then used to generate universal short time-step g-functions, which the authors labeled g*-functions.

Although the thermal capacity is considered in all of the above-mentioned numerical models, thermal interactions between pipes is not considered.

Li and Lai (2013) proposed the infinite composite-medium line source (ICMLS) solution, in which every pipe is modeled as a line source of infinite length within the grout volume. This model ignores the impact of the heat capacity of the fluid flowing through the pipes.

A simplification of a single U-tube borehole as two half pipes and divided the grout and the soil as two symmetrical parts was proposed by Beier (2014), called a complex model of infinite composite-medium cylindrical source (ICMCS). This model has a great accuracy with considering non-linear fluid temperature distribution. Thermal capacity is considered in this work.

Analogy between electrical networks and thermal conduction in the borehole is used due to its simplicity and accuracy for simulating the heat transfer into GHE. The Capacity Resistance Model (CaRM) is developed by De Carli et al. (2010) for different types of BHE configurations. For short time period, this method was extended by Zarella et al. (2011).

A Thermal Resistance and Capacitance (TRC) model was developed by Bauer et al. (2011). For single U-tube boreholes, the grout is divided into two zones, representing half of the grout volume. Grout nodes, with thermal capacitances, are added to the circuit of thermal resistances governing the heat transfer between the fluid circulating in the pipes and the borehole wall. Negative values for the short-circuit thermal resistances can be calculated when constructing the TRC model. Bauer et al. (2011) informed that the negative values do not contradict the second law of thermodynamics. However, a negative value of the resistance has an impact on the numerical stability and prediction accuracy of the model.

Pasquier and Marcotte (2012) extended the ideas from Bauer et al. (2011) integrating the thermal capacities of the heat carrier fluid and pipe and to better account for the spacing between the pipes by solving a 2D TRC model. The fluid temperature distribution along the GHE can then be evaluated by discretizing the borehole into segments, each modeled with a TRC network (Pasquier & Marcotte, 2014). Minaei and Maerefat (2017) developed an analytical model with the TRC model to calculate the short time step response of the GHE. The heat balance equations inside the borehole are derived from the equivalent thermal network model. A new equivalent thermal network is proposed inside the borehole to eliminate the negative thermal resistance in the model proposed by Bauer et al. (2011).

A finite element analysis (FEA) model coupled with TRC model was developed to validate TRC models (Diersch, Bauer, Heidemann, Rühaak, & Schätzl, 2010). However, FEA simulations are not considered suitable for engineering applications because the calculations are expensive in time domain.

This paper establishes a new hybrid model to evaluate fluid temperature profiles and heat transfer in a GHE with the U-pipe simplified as a single equivalent pipe considering equivalent thermal capacity and non-linear fluid temperature distribution. First, a 1D numerical model is constructed for radial heat transfer in the soil, grout and equivalent pipe by constructing a weighted solution from weak formulation of the unsteady heat conduction problem. Then, the model is coupled to the nonlinear temperature distribution of the fluid and inherent thermal interference between two legs of the U-tube (Zeng, Diao, & Fang, 2003). The average fluid temperature is used to calculate the inlet and outlet temperatures. The experimental data of Beier et al. (2011) is used to validate the model.

Model

Figure 1 shows a single U-tube borehole and Figure 2 shows the horizontal cross section of the borehole. The borehole is constructed by inserting the U-tube, typically HDPE, into a drilled hole of length H and radius r_b and backfilled with grout material. The two pipes of the U-tube have the same inner radius r_i and outer radius r_o, and are symmetrically positioned around the axis of the borehole.

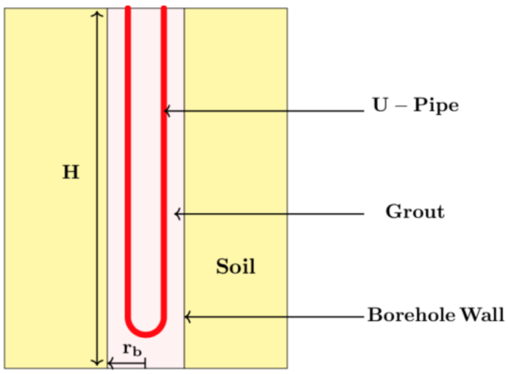

Figure 1: Sideview of a single U-tube GHE

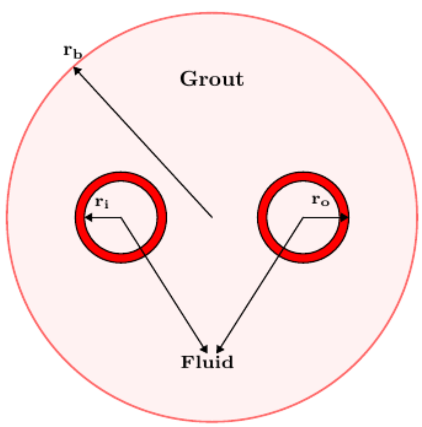

Figure 2: Cross section of the GHE

Numerical model of the equivalent pipe configuration

Using the assumption of an equivalent pipe, the single U-tube GHE is simplified by a single equivalent pipe, as shown in Figure 3.

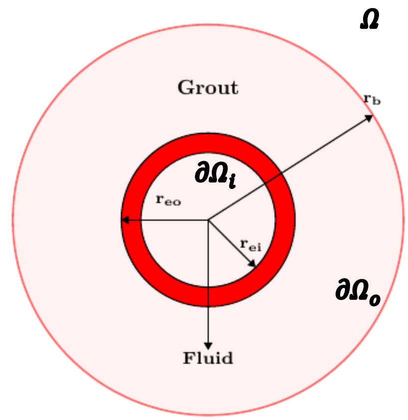

Figure 3: Equivalent pipe configuration

Fluid is located within the pipe (i.e. at $r < r_{ei}$), the equivalent pipe separates the fluid from the grout (i.e. at $r_{ei} < r < r_{eo}$), the grout extends to the borehole wall (i.e. at $r_{eo} < r < r_b$), and the soil extends outwards from the borehole wall (i.e. at $r > r_b$).

Following Lamarche (2015), the equivalent pipe geometry is given by:

$$r_{eo} = r_e e^{-2\pi k_g\left(R_b - \frac{1}{4\pi r_i h} - \frac{1}{4\pi k_p}\ln\left(\frac{r_o}{r_i}\right)\right)} \quad (1)$$

$$r_{ei} = r_{eo}\sqrt{\frac{r_i}{r_o}} \quad (2)$$

$$\rho_{ep} C_{p_{ep}} = \frac{2\left(r_o^2 - r_i^2\right)}{r_{eo}^2 - r_{ei}^2}\, \rho_p C_{p_p} \quad (3)$$

$$\rho_{eg} C_{p_{eg}} = \frac{r_b^2 - 2r_o^2}{r_b^2 - r_{ep}^2}\, \rho_g C_g \quad (4)$$

where $(\rho_{ep}, C_{p_{ep}}, k_p)$, $(\rho_{eg}, C_{p_{eg}}, k_g)$ and (ρ_s, C_{p_s}, k_s) are the density, specific heat and thermal conductivity of equivalent pipe, equivalent grout and soil respectively, (ρ_p, C_{p_p}, k_p), $(\rho_{gg}, C_{p_g}, k_g)$ and are the density, specific heat and thermal conductivity of pipe and grout, and R_b is the cross-sectional borehole thermal resistance.

These assumptions are based on equivalent volumetric heat capacities for the grout and the pipe, and an equivalent radius for U-type pipe obtained by inversion of the Laplace domain for inner and outer surface. The outer radius is chosen to preserve the borehole thermal resistance and the inner radius is chosen to preserve the tube resistance.

Considering heat conduction in the equivalent pipe configuration with constant and uniform thermal properties in each of the pipe, grout and ground, the unsteady heat conduction equation is given by:

$$\frac{\partial T}{\partial t} = \left(\frac{k}{\rho C_p}\right)_r \nabla^2 T \text{ in } \Omega \times (0, t) \quad (5)$$

where Ω is the complete domain and $\partial\Omega$ the boundary in Figure 3. The problem is one dimensional (polar coordinates) due to the axial symmetry of the domain. However, for illustration purposes, the gradient notation in eq. (5) will be used to develop the solution. The coefficient of the right side in the diffusion term becomes a function defined as follows:

$$\left(\frac{k}{\rho C_p}\right)_r = \begin{cases} \frac{k_p}{\rho_{eq} C_{peq}} & (r_{ei} < \mathrm{r} < r_{eo}) \\ \frac{k_g}{\rho_{eg} C_{peg}} & (r_{eo} < \mathrm{r} < r_b) \\ \frac{k_s}{\rho_s C_{p_s}} & (r_b < \mathrm{r} < r_s) \end{cases} \quad (6)$$

To solve the problem in eq. (5) the transient term is expressed as a Forward Finite Difference:

$$\frac{\partial T}{\partial t} \approx \frac{T^{n+1} - T^n}{\Delta t}$$

$$T^{n+1} = \Delta t \left(\frac{k}{\rho C_p}\right)_r \nabla^2 T^{n+1} + T^n \quad (7)$$

To construct the weak solution, eq. (7) is multiplied by a function w that vanishes at the boundary of Ω and is then integrated over :

$$\int_\Omega T^{n+1} w d\Omega = \int_\Omega \Delta t \left(\frac{k}{\rho C_p}\right)_r \nabla^2 T^{(n+1)} w d\Omega + \int_\Omega T^n w d\Omega \quad (8)$$

Applying the Gauss theorem to the first term of the right side of eq. (7):

$$\int_\Omega T^{n+1} w d\Omega = \int_{\partial\Omega} \Delta t \left(\frac{k}{\rho C_p}\right)_r w \frac{\partial T^{n+1}}{\partial \vec{n}} \, dA - \int_\Omega \Delta t \left(\frac{k}{\rho C_p}\right)_r \nabla w \cdot \nabla T^{n+1} d\Omega + \int_\Omega T^n w d\Omega \quad (9)$$

where $\nabla T \cdot \vec{n} = \frac{\partial T}{\partial \vec{n}}$ is the gradient normal to the boundary $\partial\Omega$.

Eq. (9) admits the construction of T by means of the Sturm-Liouville method (see (Ostrowski, 2012) and (Articolo, 2009)). Instead of constructing the complete solution of eq. (5), the solution provided in (Delouei, Emamian, Karimnejad, Sajjadi, & Tarokh, 2019) of $T(r, t)$ for spatial separation is used. For the transient term, and iterative process is defined by the initial condition and the finite difference scheme coupled with eq. (9). The complete solution requires boundary and initial conditions.

A convection boundary condition is applied at the inner surface of the equivalent pipe:

$$-2\pi r_{ei} k_p \left.\frac{\partial T^{n+1}}{\partial \vec{n}}\right|_{r=r_{ei}} = 4\pi r_i \mathrm{h} \left(T_f^{n+1} - T^{n+1}(r_{ei})\right) \quad (10)$$

$$(t > 0)$$

The temperature of the fluid is obtained from an energy balance:

$$\frac{\dot{Q}}{H} = 2\pi r_i^2 \rho_f C_{p_f} \frac{T_f^{n+1} - T_f^n}{\Delta t} + 4\pi r_i \mathrm{h} \left(T_f^{n+1} - T^{n+1}(r_{ei})\right) \quad (11)$$

$$(t > 0)$$

where T_f^{n+1} is the average fluid temperature; h is the convection coefficient (Incropera, DeWitt, Bergman, & Lavine, 2007).

For turbulent flow:

$$h = 0.023 \frac{k_f}{2r_i} Re^{0.8} Pr^{0.3}, (Re > 10000) \quad (12)$$

where Re is the Reynolds number and Pr is the Prandtl number.

A uniform initial temperature, equal to the undisturbed ground temperature, is imposed throughout the domain:

$$T_f^0 = T^0(r) = T_0 \quad (13)$$

Continuity of heat transfer rate and temperature is enforced at each of the interfaces between materials. Eq. (9) naturally satisfies these boundary conditions as the diffusion coefficient is defined in eq. (6).

Fluid temperatures along the GHE

The model given by eq. (9) allows to calculate the average wall temperature, $T^{n+1}(r_b)$, and the average temperature of the fluid, T_f^{n+1}. In this section, analytical formulations are developed to calculate T_{in} and T_{out}.

For thermal interactions between pipes of the GHE, the axial fluid temperature profiles of Zeng et al. (2003) are considered. However, the model proposed in their work is only valid for the steady state heat transfer model with constant wall temperature. In the present work, the 1D unsteady heat transfer model of the previous section is coupled to an axial discretization of the GHE, matching the average fluid temperatures of the unsteady model and the Zeng et al. (2003) solution. This setup provides the short-term effect due to the thermal capacity. The GHE is evenly divided into S segments. The bottom end of each of the segments has a depth $z_m = \frac{H \cdot m}{S}$, where $0 \leq m \leq S$, as shown in Figure 4.

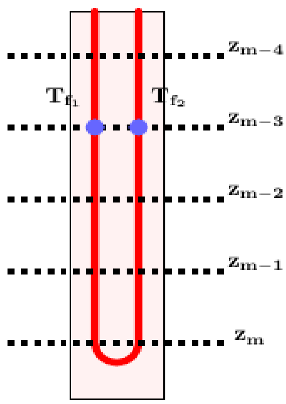

Figure 4: Vertical discretization of the GHE

The fluid temperature profiles along the U-tube pipes are given by :

$$T_{f_1}^{n+1}(z_m) = T^{n+1}(r_b) + \theta_1(z_m)\left(T_{in} - T^{n+1}(r_b)\right) \quad (14)$$

$$T_{f_2}^{n+1}(z_m) = T^{n+1}(r_b) + \theta_2(z_m)\left(T_{in} - T^{n+1}(r_b)\right) \quad (15)$$

where T_{f1}^{n+1} and T_{f2}^{n+1} are the fluid temperatures along the descending and ascending pipes, θ_1 and θ_2 are functions obtained from the solution to the steady state heat transfer within the borehole, given by :

$$\theta_1(z_m) = \cosh\beta z_m - \frac{1}{\beta S_{12}}\left[\left(\frac{S_{12}}{S_1}+1\right) - \frac{\beta S_1 \cosh\beta - 1}{\beta S_1 \cosh\beta + 1}\right]\sinh\beta z_m \quad (16)$$

$$\theta_2(z_m) = \frac{\beta S_1 \cosh\beta - 1}{\beta S_1 \cosh\beta + 1}\cosh\beta z_m - \frac{1}{\beta S_{12}}\left[1 - \left(\frac{S_{12}}{S_1}+1\right)\frac{\beta S_1 \cosh\beta - 1}{\beta S_1 \cosh\beta + 1}\right]\sinh\beta z_m \quad (17)$$

where S_1, S_{12} and β are calculated as follows:

$$S_1 = \frac{\dot{m}C_{pf}}{H}(R_{11} + R_{22}) \quad (18)$$

$$S_{12} = \frac{\dot{m}C_{pf}}{H}\frac{(R_{11}^2 - R_{13}^2)}{R_{13}} \quad (19)$$

$$\beta = \sqrt{\frac{1}{S_1^2} + \frac{2}{S_1 S_{12}}} \quad (20)$$

The thermal resistances R_{11}, R_{13} and R_{22} are calculated from the zeroth order multipole approximation as in the work of Hellström (1991).

The average fluid temperature along the length, H, at each leg of the GHE is calculated as follows:

$$\sum_{m=0}^{S} T_{f_1}^{n+1}(z_m) = (s+1)T^{n+1}(r_b) + \sum_{m=0}^{S} \theta_1(z_m)\left(T_{in} - T^{n+1}(r_b)\right) \quad (21)$$

$$\sum_{m=0}^{S} T_{f_2}^{n+1}(z_m) = (s+1)T^{n+1}(r_b) + \sum_{m=0}^{S} \theta_2(z_m)\left(T_{in} - T^{n+1}(r_b)\right) \quad (22)$$

The average fluid temperature along the pipes is equal to the average fluid temperature in the equivalent pipe, T_f^{n+1}, calculated by eqs. (11) and (9) :

$$T_f^{n+1} = \frac{1}{2(S+1)}\left[\sum_{m=0}^{S} T_{f_1}^{n+1}(z_m) + \sum_{m=0}^{S} T_{f_2}^{n+1}(z_m)\right] \quad (23)$$

Combining eqs. (21), (22) with (23), the inlet temperature of the GHE is given by :

$$T_{in} = T^{n+1}(r_b) + \frac{2(S+1)\left(T_f^{n+1} - T^{n+1}(r_b)\right)}{\sum_{m=0}^{S}\left(\theta_1(z_m) + \theta_2(z_m)\right)} \quad (24)$$

The thermal energy balance $\dot{Q} = \dot{m}C_{pf}(T_{out} - T_{in})$ is applied to calculate the outlet temperature, T_{out}. While eq. (15) enables the calculation of a fluid temperature in the upward flowing pipe at $z_m = 0$, the resulting temperature would present a mismatch with the outlet fluid temperature predicted from the thermal energy balance since the profiles of Zeng et al. (2003) consider steady-state heat transfer. The outlet temperature is then defined by :

$$T_{out} = T_{in} - \frac{\dot{Q}}{\dot{m}C_{pf}} \quad (25)$$

Results and discussion

Lagrangian 1st order polynomials are used for the function w of eq. (5) in the complete domain discretized part-by-part. In this case $\Delta t = 10$ secs. Discretization is performed in eq. (5) by means of eq. (9) using the Sturm-Liouville solution technique. A quadrature method by Gauss-Legendre technique is used to solve the integrals.

The experimental data set of Beier et al. (2011) is used to verify the validity of the complete model. In this case, the uninterrupted test was chosen. In their experiment, a 18.3 m long borehole is placed horizontally in a square sandbox with a side length of 1.8 m. A constant heat rate is apply over a period of 52 h while the fluid flow rate is maintained constant. The heat injected is measured from the electrical heater used to provide heat while fluid temperatures are measured from thermistors.

For a cross validation, a tridimensional FEA model was implemented, akin to the finite element model proposed by Diersch et al. (2011). Figure 5 shows the tridimensional grid of triangular prismatic elements used for the simulations. The pipes and grout are modeled as line elements. Four lines were discretized for inlet, outlet fluid temperature and left grout and right grout, using the TRC model of Bauer et al. (2011). The model consists of 6498 nodes and 11236 prismatic elements. For interpolation between elements, lagrangian 2nd order polynomials are applied. For accelerated convergence, a preconditioning algorithm was used (Takami, Matsui, Oka, & Iijima, 2018).

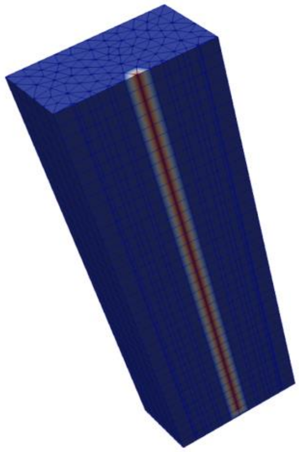

Figure 5: Grid of the finite element model

Table 3 shows the parameters used for both the present and the FEA simulation.

Table 3: Parameters

Parameters	Value
r_b	0.063 m
H	18.3 m
r_i	0.01367 m
r_o	0.0167 m
k_p	0.39 W/mK
$(\rho C_p)_p$	2.2×10^6 J/m^3K
k_g	0.73 W/mK
$(\rho C_p)_g$	3.8×10^6 J/m^3K
k_s	2.82 W/mK
$(\rho C_p)_s$	2×10^6 J/m^3K
k_f	0.613 W/mK
$(\rho C_p)_f$	4.17×10^6 J/m^3K
C_{pf}	4180 mK/W
T_0	22 °C
$\dot{Q}$	1056 W
$\dot{m}$	0.196 kg/s
R_b	0.158 mK/W

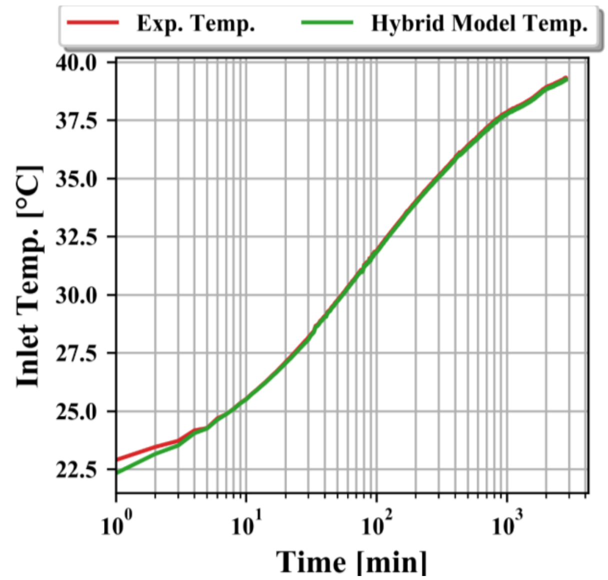

Figure 6: Inlet Temperature

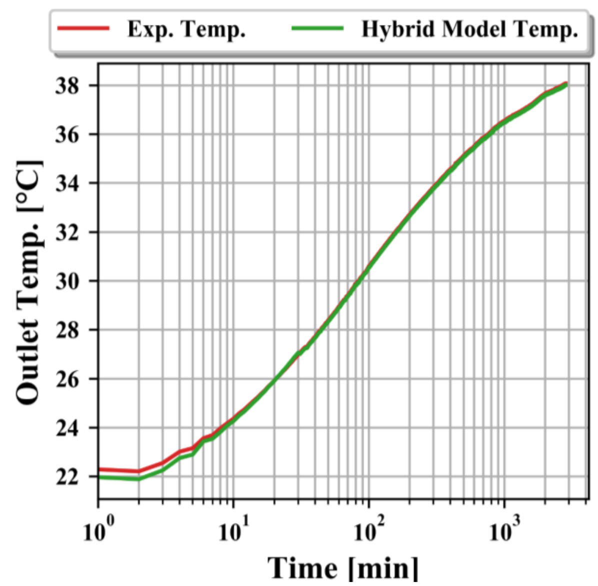

Figure 7: Outlet Temperature

Figure 6 and 7 show the predicted and measured fluid temperatures at the inlet and outlet of the GHE, respectively. In the first 10 min of simulation, it can be seen that there is a maximum difference of 0.19°C between experimental result and simulation. Figure 8 shows the temperature distribution around the equivalent pipe after 2 h of heat injection.

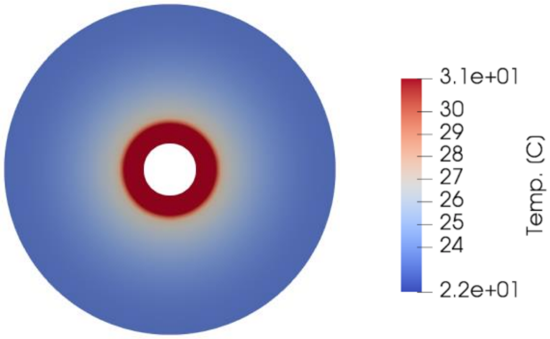

Figure 8: Temperature distribution of Equivalent GHE

Table 4 presents the RMSE for the hybrid model and the FEA simulation. It can be seen that both the proposed method and the FEA simulation are consistent with the experimental data. As previously mentioned, while FEA analysis allows the complete GHE to be simulated with high precision, it is rarely viable for engineering purposes. In the present case, the FEA simulation of the experiment of Beier et al. (2011) required 50 min of computation time, while the proposed hybrid model required 10 min. Both simulations were performed on a MacBook 2015 equipped with 8GB RAM and a 1.1GHz Intel M processor.

Table 4: RMSE for inlet and outlet temperature

	Inlet T.	**Outlet T.**
Hybrid Model	0.1	0.07
FEA Simulation	0.32	0.21

Conclusions

A new heat transfer model for U-tube pipe was developed, which includes two parts. The first part simplifies the U-tube pipes using the assumption of a single equivalent pipe, with the heat transfer in the pipe-grout-soil calculated from the heat equation in weak formulation (eq. (9)). The solution to this 1D numerical model returns the average fluid temperature within the GHE. The second part is based on an analytical solution to the non-linear distribution of the fluid temperature based on a quasi-3D model. Coupled with the numerical model developed in the first part, the inlet and outlet fluid temperatures are evaluated as functions of the average fluid temperature and borehole wall temperature.

The model presented in this work shows a good agreement with the experimental results for short time simulations. This model allows to vary mass flow rate, heat flux and convective coefficient. The versatility of the grid generation allows to manage different types of U-tube pipes due to the uncoupled grid for the weighted solution of eq. (9). This method requires to solve, at each time step, a system of integro-differential equations to evaluate the temperatures at the next time step by means of a finite difference method and an M-point quadrature method. However, this method is always stable and convergent.

For further research, the numerical model will be extended to a two-dimensional model to consider the variations of the temperature along the length of the borehole. The numerical model will be used as a benchmark to verify the accuracy of short-time analytical models of the GHE. Equation (8) allows to discretizes (1) using Finite Element Method or Finite Volume Method. However, the advantage of the method proposed here is that T does not depend spatially of the discretization of the domain due to fact the construction of the solution with Sturm-Liouville procedure.

Acknowledgement

This study is funded by the Natural Sciences and Engineering Research Council of Canada (NSERC) [grant number: RGPIN-2018-04471]

References

Articolo, G. (2009). The Diffusion or Heat Partial Differential Equation. In G. Articolo, *Partial Differential Equations & Boundary Value Problems with Maple* (pp. 161-215). -: Academic Press.

Bandyopadhyay, G., Gosnold, W., & Mann, M. (2008). Analytical and semi-analytical solutions for short-time transient response of ground heat exchangers. *Energy and Buildings*, 1816-1824.

Bauer, D., Heidemann, W., & Diersch, H. (2011). Transient 3D analysis of borehole heat exchanger modeling. *Geothermics 40* , 250–260.

Bauer, D., Heidemann, W., Mu, H., & Diersch, H. (2011). Thermal resistance and capacity models for borehole heat exchangers. *Int. J. Energy Res. 35*, 312-320.

Beier, R. (2011). Vertical temperature profile in ground heat exchanger during in-situ test. *Renew. Energy 36*, 1578–1587.

Beier, R. (2014). Transient heat transfer in a U-tube borehole heat exchanger. *Appl. Therm. Eng. 62*, 256–266.

Beier, R., Smith, M., & Spitler, J. (2011). Reference data sets for vertical borehole ground heat exchanger models and thermal response test analysis. *Geothermics 40 (1)*, 79–85.

Bialecki, R., & Nowak, A. (1981). Boundary value problems in heat conduction with nonlinear material and nonlinear boundary conditions. *Applied Mathematical Modelling*, 307-904X.

Bose, J. E., Parker, J., & Faye, C. (1985). *Design/data manual for closed-loop ground-coupled heat pump systems*. Atlanta, GA: American Society of

Heating, Refrigerating, and Air-Conditioning Engineers.

Brussieux, Y., & Bernier, M. (2019). Universal short-time g*-functions: generation and application. *Science and Technology for the Built Environment*, 993-1003.

De Carli, M., Tonon, M., Zarella, A., & Zecchin, R. (2010). A computational capacity resistance (CaRM) for vertical ground-coupled heat exchangers. *Renew. Energy 35*, 1537-1550.

Delouei, A., Emamian, A., Karimnejad, S., Sajjadi, H., & Tarokh, A. (2019). On 2D asymmetric heat conduction in functionally graded cylindrical segments: A general exact solution. *International Journal of Heat and Mass Transfer*, 1-12.

Delouei, A., Kayhani, M., & Norouzi, M. (2012). Exact analytical solution of unsteady axi-symmetric conductive heat transfer in cylindrical orthotropic composite laminates. *International Journal of Heat and Mass Transfer*, 4427-4436.

Diersch, H.-J., Bauer, D., Heidemann, W., Rühaak, W., & Schätzl, P. (2010). *Finite element formulation for borehole heat exchangers in modeling geothermal heating systems by FEFLOW* (Vol. V). Berlin: DHI-WASY GmbH.

Diersch, H.-J., Bauer, D., Heidemann, W., Rühaak, W., & Schätzl, P. (2011). Finite element modeling of borehole heat exchanger systems: Part 1. Fundamentals. *Computers & Geosciences*, 1122-1135.

Gu, Y., & O'Neal, D. (1998). Development of an equivalent diameter expression for vertical U-Tubes used in ground-coupled heat pumps. *ASHRAE Transactions*, 347-355.

Hellström, G. (1991). *Ground heat storage, Thermal analysis of duct storage systems*. Lund, Sweden: Doctoral Thesis, Department of Mathematical Physics.

Incropera, F., DeWitt, D., Bergman, T., & Lavine, A. (2007). *Fundamentals of Heat and Mass Transfer* (sixth ed.). New York: John Wiley & Sons Inc.

Javed, S., & Claesson, J. (2011). New analytical and numerical solutions for the short-term analysis of vertical ground heat exchangers. *ASHRAE Trans. 117*, 3-12.

Lamarche, L. (2013). Short-term behavior of classical analytic solutions for the design of ground-source heat pumps. *Renew. Energy 57*, 171-180.

Lamarche, L. (2015). Short-time analysis of vertical boreholes, new analytic solutions and choice of equivalent radius. *Int. J. Heat Mass Transf. 91*, 800–807.

Li, M., & Lai, A. (2013). Analytical model for short-time responses of ground heat exchangers with U-shaped tubes: model development and validation. *Appl. Energy 104*, 510-516.

M. Li, P. L., Chan, V., & Lai, A. (2014). Full-scale temperature response function (G- function) for heat transfer by borehole ground heat exchangers (GHEs) from sub- hour to decades. *Appl. Energy 136* , 197–205.

Minaei, A., & Maerefat, M. (2017). A new analytical model for short-term borehole heat exchanger based on thermal resistance capacity model. *Energy and Buildings*, 233-242.

Nian, Y., & Cheng, W. (2018). Analytical g-function for vertical geothermal boreholes with effect of borehole heat capacity. *Appl. Therm. Eng. 140*, 733–744.

Ostrowski, P. (2012). Unidirectional and stationary heat conduction problem in two- phase hollow cylinder with functionally graded and temperature dependent effective material properties. -, -.

Pasquier, P., & Marcotte, D. (2012). Short-term simulation of ground heat exchanger with an improved TRCM. *Renew. Energy*, 92-99.

Pasquier, P., & Marcotte, D. (2014). Joint use of quasi-3D response model and spectral method to simulate borehole heat exchanger. 281-299.

Shonder, J., & Beck, J. (1999). Determining effective soil formation thermal properties from field data using a parameter estimation technique. *Build. Eng.*, 458-466.

Stehfest, H. (1970). Remark on algorithm 368: Numerical inversion of laplace transforms. *Commun. ACM*, 47-49.

Takami, T., Matsui, S., Oka, M., & Iijima, K. (2018). A numerical simulation method for predicting global and local hydroelastic response of a ship based on CFD and FEA coupling. *Marine Structures*, 368-386.

Xu, X., & Spliter, J. (2006). Modeling of Vertical Ground Loop Heat Exchangers with Variable Convective Resistance and Thermal Mass of the Fluid. *Proceedings of Ecostock* (pp. -). America: Pomona.

Yavuzturk, C., & Spitler, J. (1999). A Short Time Step Response Factor Model for Vertical Ground Loop Heat Exchangers. *ASHRAE Transactions*, 475-485.

Zarrella, A., Scarpa, M., & De Carli, M. (2011). Short time step analysis of vertical ground-coupled heat exchangers: The approach of CaRM. *Renewable Energy*, 2357-2367.

Zeng, H., Diao, N., & Fang, Z. (2003). Heat transfer analysis of boreholes in vertical ground heat exchangers. *Int. J. Heat Mass Transf. 46*, 4467–4481.

Zhang, C., Guo, Z., Liu, Y., & X. Cong, D. P. (2014). A review on thermal response test of ground-coupled heat pump systems. *Renew. Sustain. Energy Rev. 40*, 851–867.